Toluene Disproportionation and Methylation over Zeolites TNU-9, SSZ-33, ZSM-5, and Mordenite Using Different Reactor Systems

ARTICLE *in* INDUSTRIAL & ENGINEERING CHEMISTRY RESEARCH · FEBRUARY 2011

Impact Factor: 2.59 · DOI: 10.1021/ie1018904

3 AUTHORS:

Taiwo Odedairo
University of Queensland
34 PUBLICATIONS **159** CITATIONS
SEE PROFILE

Rabindran Jermy
King Fahd University of Petroleum and Mine…
45 PUBLICATIONS **578** CITATIONS
SEE PROFILE

Sulaiman al-khattaf
King Fahd University of Petroleum and Mine…
117 PUBLICATIONS **1,120** CITATIONS
SEE PROFILE

I&EC research
Industrial & Engineering Chemistry Research

ARTICLE

pubs.acs.org/IECR

Toluene Disproportionation and Methylation over Zeolites TNU-9, SSZ-33, ZSM-5, and Mordenite Using Different Reactor Systems

T. Odedairo, R.J. Balasamy, and S. Al-Khattaf*

Center of Excellence in Petroleum Refining and Petrochemicals, King Fahd University of Petroleum and Minerals, Dhahran 31261, Saudi Arabia

ABSTRACT: An array of zeolites varying in the channel structural design and acidity was investigated in toluene methylation with methanol, together with toluene disproportionation, using fluidized-bed and fixed-bed reactors. The conversions of toluene in the methylation and disproportionation reactions in the fixed-bed reactor were higher than those in the fluidized-bed reactor over the zeolite based catalysts at similar reaction conditions. The unique pore architecture of zeolite TNU-9, with 10-ring channel systems, being slightly larger zeolite compared with ZSM-5, can offer new opportunities for toluene disproportionation, as well as for toluene methylation. The medium pore zeolite TNU-9 was found to possess the highest conversion in toluene disproportionation as compared with other zeolite based catalysts under study. In toluene methylation, the highest toluene conversion was achieved with mordenite based catalyst (MOR-A), while the xylene selectivity follows the order: ZSM-5 > TNU-9 > MOR-A > SSZ-33 > MOR-B. This order indicates that xylene selectivity is directly related to the size of channels from medium to large pore zeolites. Using the fluidized bed, the apparent activation energies for toluene methylation follow the order: ZSM-5 (46.8 kJ/mol) > TNU-9 (33.9 kJ/mol) > MOR-B (13.9 kJ/mol) ≈ MOR-A (13.1 kJ/mol) > SSZ-33 (8.2 kJ/mol).

1. INTRODUCTION

Zeolites represent the most important inorganic materials for catalysis, finding applications in dozens of technological processes from petroleum refining and petrochemistry up to fine chemical synthesis.[1,2] Zeolites were first introduced as acid catalysts for oil refining in the late 60s, improving the catalytic behavior of the previous amorphous silica−alumina.[3−6] The individual types of zeolites differ in the size of the channels (8-, 10-, 12-, 14-, or even larger rings), connectivity of the channels, and the presence or absence of cages in channel intersections or along the channel itself.[7] There are two major reasons for a high significance of zeolites in transformations of aromatic hydrocarbons. At first, all transformations of aromatic hydrocarbons including various alkylation, isomerization, disproportionations, and transalkylations are catalyzed at industrial scale by zeolites. Second, zeolites serve at laboratory scale as ideal model catalysts for comparing their catalytic behavior in aromatic transformations.[8−14]

Alkylbenzenes undergo isomerization, disproportionation, alkylation, and transalkylation reactions over numerous catalysts exhibiting Bronsted and Lewis acidity. As is well-known, the benzene is a key raw material for many intermediates of petrochemicals, and the xylenes are important starting materials for the production of synthetic fibers, plasticizers, and resin. The convenient ways to get more valuable benzene and xylenes from surplus toluene and trimethylbenzenes consists of the processes such as toluene disproportionation,[15] toluene alkylation with methanol,[16] or toluene disproportionation and transalkylation with trimethylbenzenes.[17] In the process of toluene alkylation with methanol, main coreactions are toluene disproportionation, the further alkylation of xylene with methanol, and the conversion of methanol to hydrocarbons at high temperatures.[18] The hastily growing demand for benzene and xylenes urges development of all stated processes above.

Both large and medium-pore zeolites possessing 12- and 10-ring pore apertures such as Beta,[19] USY,[20] mordenite,[21] ITQ-7,[22] and ZSM-5[12] are potential solid acid catalysts for interconversion of alkylbenzenes into xylenes. The activity and selectivity of SSZ-33 based catalyst was studied in comparison with other zeolites in toluene disproportionation.[23] SSZ-33 catalyst gave the highest toluene conversion as compared with other zeolite catalysts. The authors attributed the high toluene conversion of SSZ-33 catalyst to its high acidity together with increased mass transport through large pores. The kinetics of toluene disproportionation was investigated over fresh and coked H-mordenite.[24] Two stages of deactivation mechanism were derived. Pore plugging and deactivation by coke predominates the initial coking period at ca. 7% coke content; during that period, the strong Bronsted acid site diminishes and also the pore voidage shrinks. The disproportionation of toluene was recently studied by Zilkova et al.[11] over different zeolite catalysts. The authors found that the conversion of toluene over the zeolite catalysts cannot be directly related to the increasing pore size or connectivity of individual zeolite channels. Also, the methylation of toluene with methanol has been reported over three different zeolite catalysts (H-ZSM-5, H-mordenite, and H-beta).[25] Polymethylbenzenes larger than *p*-xylene were found to experience severe diffusional limitations in H-ZSM-5 channels. The catalytic activity of SSZ-33 based catalyst has also been studied in alkylation of toluene with methanol.[26] The

Received: September 13, 2010
Accepted: January 14, 2011
Revised: December 3, 2010
Published: February 08, 2011

dx.doi.org/10.1021/ie1018904 | *Ind. Eng. Chem. Res.* 2011, 50, 3169–3183

authors reported xylenes have the most predominant product, followed by trimethylbenzenes and other alkylaromatics of high molecular weight in substantially lower amounts. Recently, Rabiu and Al-Khattaf[12] investigated the methylation of toluene over fresh and precoked ZSM-5 based catalyst. The authors reported average apparent activation energy for toluene methylation over the fresh ZSM-5 catalyst to be ~67.79 kJ/mol.

Investigating the catalytic activity of a new three-dimensional zeolite, TNU-9, with 10-ring channel systems, being rather similar to the industrially most frequently employed ZSM-5, with mordenite, SSZ-33, and ZSM-5 in methylation and disproportionation reaction of toluene and determining the effect of the zeolite properties (channel structural design, acidity) on these reactions are the main objectives of this study. Both reactions were investigated in the gas phase in a fixed-bed reactor and a fluidized-bed reactor. In addition, a comprehensive kinetic modeling of toluene methylation over the different zeolite based catalysts with catalyst deactivation model based on time-on-stream will be developed. Up-to-date, the kinetic study over TNU-9 and SSZ-33 based catalyst in the methylation of toluene with methanol has not been reported in the open literature. The proposed model will be tested with the obtained experimental data, and the model parameters will be estimated using nonlinear regression analysis.

2. EXPERIMENTAL SECTION

2.1. Preparation of Catalysts. The uncalcined proton form of mordenite (H-mordenite) zeolite (HSZ-690HOA) used in this work was obtained from Tosoh Chemicals, Japan. The parent mordenite zeolites have silica to alumina ratio of 180 and 18.3, for mordenite-A (MOR-A) and mordenite-B (MOR-B), respectively. An alumina binder (Cataloid AP-3) contains 75.4 wt % alumina, 3.4% acetic acid, and water as a balance. The alumina binder was obtained from CCIC Japan. The alumina binder was dispersed in water and stirred for 30 min to produce thick slurry. The zeolite powder was then mixed with alumina slurry to produce a thick paste. The composition of the zeolite based catalyst in weight ratio is as follows: mordenite/AP-3 (2:1). The uncalcined proton form of ZSM-5 (CT-405) used in this study was obtained from CATAL, UK. The parent ZSM-5 has silica to alumina ratio of 30. A similar procedure used for the preparation of the mordenite based catalyst used in this study was also followed for the preparation of the ZSM-5 based catalyst. The composition of the ZSM-5 zeolite based catalyst in weight ratio is as follows: ZSM-5/AP-3 (2:1). Zeolite SSZ-33 and TNU-9 and their characterization data (X-ray diffraction (XRD), not provided in the text, scanning electron microscopy (SEM), Fourier transform infrared spectroscopy (FTIR)) used in this study were obtained from J. Heyrovsky Institute of Physical Chemistry, Academy of Science of the Czech Republic, Prague, Czech Republic. The parent SSZ-33 has Si/Al ratio of 18, while the parent TNU-9 has Si/Al ratio of 21.9. The synthesis method used for the preparation of SSZ-33 can be found in Al-Khattaf et al.[23] Alumina was added to these zeolites (SSZ-33 and TNU-9) adopting the same procedure used for mordenite and ZSM-5 based catalyst.

2.2. Characterization of Catalysts. Surface areas were obtained from N_2 physical adsorption isotherms by applying the Brunauer−Emmett−Teller (BET) method with Quantachrome AUTO-SORB-1 (model # ASI-CT-8). The samples were preheated at 100 °C for 3 h in flowing N_2. Type and concentration of acid sites in all zeolites were determined by adsorption of pyridine as probe molecules followed by FTIR spectroscopy (Nicolet 6700 FTIR) using the self-supported wafer technique. Prior to adsorption, self-supporting zeolite wafers were activated in situ by evacuation at a temperature of 450 °C overnight. Adsorption of pyridine proceeded at 150 °C for 20 min at a partial pressure of 5 Torr.

The concentrations of Bronsted and Lewis acid sites were calculated from the integral intensities of individual bands characteristic of pyridine on Bronsted acid sites at 1550 cm^{-1} and the band of pyridine on Lewis acid sites at 1455 cm^{-1} and molar absorption coefficient[27] of $\varepsilon(B) = 1.67 \pm 0.1$ cm μmol^{-1} and $\varepsilon(L) = 2.22 \pm 0.1$ cm μmol^{-1}, respectively. The infrared spectra of absorbed pyridine on SSZ-33 were recently discussed in detail by Gil et al.[28] Crystallinity of all zeolites under study were determined by powder X-ray diffraction (XRD) with a Bruker D8 Advance X-ray powder diffractometer equipped with a graphite monochromator and position sensitive detector using Cu Kα radiation in Bragg−Brentano geometry. X-ray powder patterns of all zeolites exhibited good crystallinity and characteristic diffraction lines. The shape and size of all zeolites were determined by scanning electron microscopy (Jeol, JSM-5500LV).

2.3. Catalytic Reactions. Toluene disproportionation and methylation with methanol were investigated in the gas phase in a fixed-bed and a fluidized-bed reactor. The fixed-bed reactor (ID 0.25 in., model # 401C-0286, Autoclave engineers) was employed for toluene methylation and disproportionation reactions using 400 mg of catalyst sample for each run. Analytical grade (99% purity) pure toluene and methanol were obtained from Sigma-Aldrich. All chemicals were used as received, and no attempt was made to further purify the samples. The feed molar ratio of toluene to methanol is 1:1. The catalyst was pretreated in H_2 flow at 400 °C for 1 h before each run. After pretreatment, the temperature was lowered to the reaction temperature and the feedstock was fed into the H_2 stream using a high pressure feeding pump. The liquid feedstock (toluene + methanol) was passed through an oven kept at 150 °C, where it was preheated, vaporized, and carried by the hydrogen gas to the reactor tube. The residence time was changed by changing the flow rates of H_2 and liquid feedstock accordingly in the range of 50−300 and 0.04−2.40 mL/min, respectively. All experiments were run at 0.907 MPa hydrogen pressure; reaction temperatures of 300, 325, 350, and 400 °C; and at six different values of residence times. Toluene disproportination alone was also carried out at the same reaction conditions.

Similarly, disproportionation and methylation of toluene with methanol was also performed in a riser simulator that mimics the operation of a fluidized-bed reactor. This reactor is bench scale equipment with internal recycle unit invented by de Lasa.[29] A detailed description of various riser simulator components, sequence of injection and sampling can be found in Kraemer.[30] Catalytic experiments were carried out in the riser simulator with a feed mixture of toluene and methanol for reaction times of 5, 10, 15, and 20 s at temperatures of 300, 350, and 400 °C, and the toluene disproportionation alone was also carried out at the same reaction conditions. About 800 mg of the fluidizable catalyst particles (60 μm average size) were weighed and loaded into the riser simulator basket. The system was then sealed and tested for any pressure leaks by monitoring the pressure changes in the system. Furthermore, the reactor was heated to the desired reaction temperature. The vacuum box was also heated to ~250 °C and evacuated to a pressure of ~0.5 psi to prevent any condensation of hydrocarbons inside the box. The heating of the riser simulator was conducted under continuous flow of inert gas (Ar),

Table 1. Characteristics of the Zeolites Used for the Study

sample code[a]	Si/Al ratio	Lewis sites (mmol/g)	Bronsted sites (mmol/g)	surface area (m^2/g)	Lewis sites (%)	Bronsted sites (%)
F.C.-ZSM-5	20.3	0.28	0.21	304	57	43
F.C.-TNU-9	19.3	0.25	0.33	330	43	57
F.C.-MOR-A	135.9	0.12	0.03	441	80	20
F.C.-MOR-B	17.0	0.25	0.23	420	52	48
F.C.-SSZ-33	13.6	0.48	0.18	448	72	28
AP-3		0.64	0	280	100	0

[a] F.C.: final catalyst.

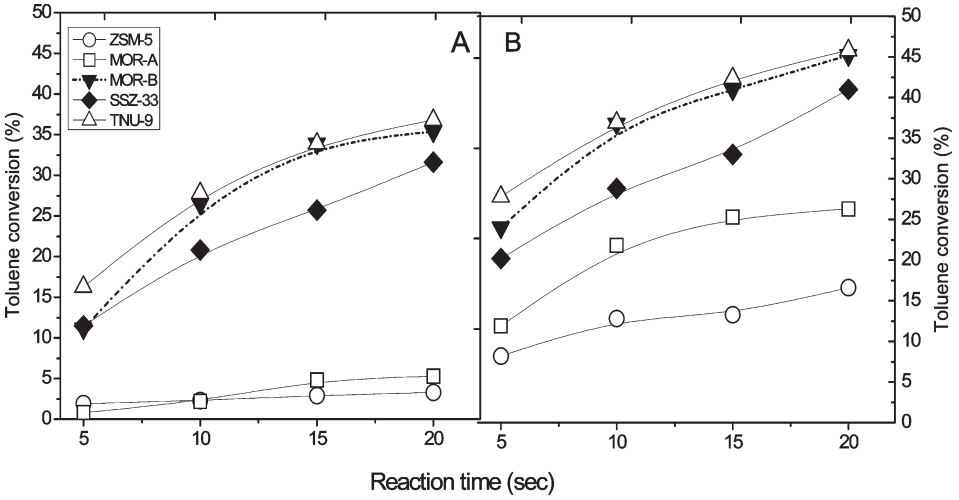

Figure 1. Effect of reaction conditions on toluene conversion in toluene disproportionation over different structural types of zeolites (reactor = fluidized-bed, catalyst/feed = 5, reaction temperature of 300 °C (A) and 400 °C (B)): (Δ) TNU-9, (▼) MOR-B, (♦) SSZ-33, (□) MOR-A, and (○) ZSM-5).

and it usually takes a few hours until thermal equilibrium is finally attained. Meanwhile, before the initial experimental run, the catalyst was activated for 15 min at 620 °C in a stream of Ar. The temperature controller was set to the desired reaction temperature, and in the same manner, the timer was adjusted to the desired reaction time. At this point, the GC is started and set to the desired conditions. Once the reactor and the gas chromatograph have reached the desired operating conditions, 0.162 g of the feedstock was injected directly into the reactor via a loaded syringe. After the reaction, the four-port valve opened immediately, ensuring that the reaction was terminated and the entire product stream was sent online to analytical equipment via a preheated vacuum box chamber. The products were analyzed in an Agilent 6890N gas chromatograph with a flame ionization detector and a capillary column INNOWAX, 60 m cross-linked methyl silicone with an internal diameter of 0.32 mm. During the course of the investigation, a number of runs were repeated to check for reproducibility in the experimental results, which were found to be excellent. Typical errors were in the range of ±2%.

3. RESULTS AND DISCUSSION

3.1. Zeolites and Catalysts Characterization. The SEM images evidence the absence of impurities including an amorphous one (not shown here). The typical SEM images of zeolites SSZ-33 and TNU-9 used in this study can be found in Odedairo and Al-Khattaf.[31] The crystal sizes of all zeolites used in this present study were between 0.3 and 1 μm. Table 1 provides the quantitative evaluation of FTIR spectra of parent zeolites and final catalysts. For application of zeolites in acid catalyzed reactions, the concentration of acid sites (Bronsted and Lewis types) is of utmost importance. The concentrations of Bronsted acid sites and all acid sites of all catalysts under study are presented in Table 1. In this case, the following sequences were obtained: TNU-9 > MOR-B > ZSM-5 > SSZ-33 > MOR-A for Bronsted sites and SSZ-33 > TNU-9 > ZSM-5 > MOR-B > MOR-A for all sites. It was observed that an increase in the concentration of Lewis acid sites was noticed after modification of parent zeolites with alumina binder.

3.2. Toluene Disproportionation. The toluene conversions in the disproportionation reaction carried out at 300 and 400 °C in the fluidized-bed reactor follow the order: ZSM-5 < MOR-A < SSZ-33 < MOR-B < TNU-9. It was observed that increasing the temperature from 300 to 400 °C did not change the order of toluene conversion (see Figure 1A,B). It is evident from Figure 1A,B that the conversions of toluene increased with increasing time and temperature to a maximum of 15.6%, 25.3%, 40.0%, 44.2%, and 44.8% at 400 °C for a reaction time of 20s over ZSM-5, MOR-A, SSZ-33, MOR-B and TNU-9 based catalysts, respectively. The order of toluene conversions noticed over the zeolite based catalysts under study does not match with the total amount of acid sites (Bronsted plus Lewis) (MOR-A < MOR-B < ZSM-5 < TNU-9 < SSZ-33). SSZ-33 based catalyst should provide the highest toluene conversions, if acid sites would be considered as a major factor for toluene conversion. Also, toluene conversions do not follow the order of the channel sizes and dimensionality.

These findings are in agreement with what was reported by Zilkova et al.[11] that there is no general and clear-cut relationship between the sizes of the pores and their channel dimensionality and toluene conversions in toluene disproportionantion. Benzene and xylenes were the major products noticed in the disproportionation reaction of toluene over ZSM-5, while a negligible amount of trimethylbenzene (TMB) was also noticed. The insignificant amount of TMBs noticed over ZSM-5 based catalyst may be as a result of the severe diffusional limitations which these polymethylbenzenes encountered and possibly transition state restrictions leading to shape selectivity.

The channel diameter in mordenite is large enough to give access to molecules with the size of trimethylbenzenes. At 350 and 400 °C, traces of TMBs were observed in the disproportionation reaction of toluene over MOR-A, while significant amounts of trimethylbenzenes were noticed over MOR-B, at all temperatures studied. Formation of trimethylbenzene over these zeolites may be as a result of secondary disproportionation of xylene isomers occurring at those temperatures. It was observed that a much higher toluene conversion was noticed in the disproportionation of toluene over MOR-B (high acidity), as compared with MOR-A which is of a lower acidity, at all temperatures studied. Similar observation was reported by Al-Khattaf[32] during the catalytic transformation of toluene over Y-zeolite based catalysts of different acidity. It was found that H−Y with high acidity gave increased toluene reactivity and better conversion than that of USY-1 catalyst with lower acidity. A slightly higher benzene yield was observed over MOR-B (12.4%) as compared with MOR-A (11.8%) at a constant conversion level of ∼25.3%. On the other hand, a slighly higher xylene yield was noticed over MOR-A (12.5%) as compared with the yield of xylene that was observed over MOR-B (10.9%), also at constant toluene conversion of ∼25.3%. A negligible amount of gaseous hydrocarbon was noticed over MOR-A, while ∼0.2% gaseous hydrocarbon was observed over MOR-B. This is consistent with what was reported by Al-Khattaf[32] that acidity in the range of 0.1−0.2 mmol/g favors the disproportionation reaction, producing more xylenes, whereas an acidity of >0.2 mmol/g favors the dealkylation reaction, producing more gases.

Zeolite SSZ-33 (CON topology) possesses a channel system complied of intersecting 12-ring and 10-ring pores and also allows formation of bulky intermediates as compared to ZSM-5 based catalyst in which mainly benzene and xylenes were formed. An insignificant amount of trimethylbenzenes was noticed at 300 °C over SSZ-33 catalyst, which indicates that toluene mainly transforms through disproportionation and that the secondary reactions are less important. A significant amount of benzene (22.9%) was noticed in the toluene disproportionation reaction over TNU-9 at 400 °C for a reaction time of 20 s. For example, the benzene yield increased from 18.5% at 300 °C to 22.5% at 350 °C and then to 22.9% at 400 °C, all at a reaction time of 20 s. The trend of the benzene yield noticed over TNU-9 is not surprising since benzene can be produced by both primary (toluene disproportionation) and secondary (xylene transalkylation) reactions.

Figure 2 presents the product selectivity during toluene disproportionation over ZSM-5, TNU-9, MOR-A, MOR-B, and SSZ-33 at constant conversion level of 16%. The selectivity to the sum of xylenes over the different zeolite catalysts under study follow the order: MOR-B < SSZ-33 < TNU-9 < ZSM-5 ≈ MOR-A. Similarly, the benzene selectivity was found in the order: MOR-A ≈ ZSM-5 < MOR-B < SSZ-33 < TNU-9. The lower selectivity

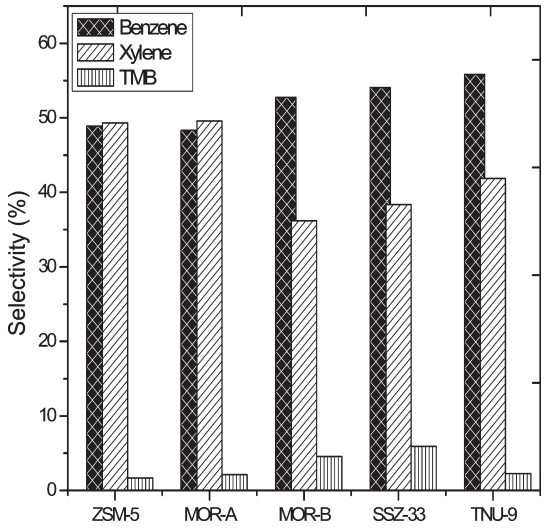

Figure 2. Product selectivity of toluene disproportionation over the different catalysts at 16% toluene conversion (toluene/methanol, 1:1 mol ratio; reactor = fluidized-bed; catalyst/feed = 5; reaction temperature: 300, 350, and 400 °C).

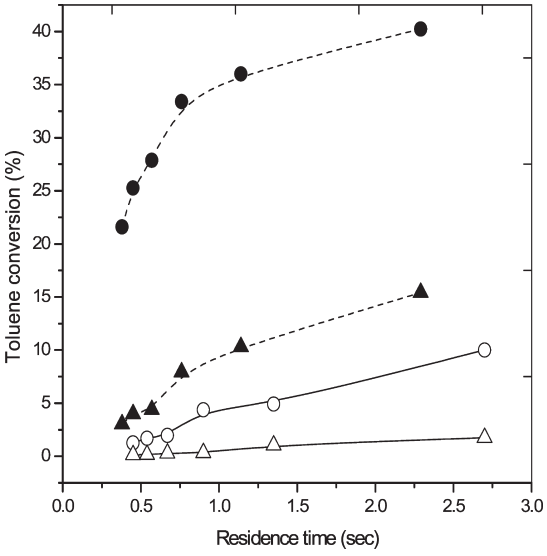

Figure 3. Effect of reaction conditions on toluene conversion in toluene disproportionation over ZSM-5 (▲, △) and SSZ-33 (●, ○) (reactor = fixed-bed; reaction temperature of 300 °C (white symbols) and 400 °C (black symbols)).

of xylenes observed over MOR-B, SSZ-33, and TNU-9 may be as a result of the rate of byproducts formation (TMBs and even tetramethylbenzenes), decreasing the selectivity toward xylenes, and may also be attributed to the void reaction space in the zeolites channel system. The xylenes/benzene molar ratios were also compared at a constant conversion level of 16% over all the catalysts, when the fluidized-bed reactor was used and the ratios were found to follow the order: MOR-A > ZSM-5 > TNU-9 > SSZ-33 > MOR-B. It can be observed that the order of xylenes/benzene ratios do not match with the order of toluene conversions. With the exception of the mordenite zeolite based catalysts (MOR-A and MOR-B), the order of xylenes/benzene ratios noticed over all the zeolite based catalysts under study indicates the increasing reaction volume provided by individual zeolites.

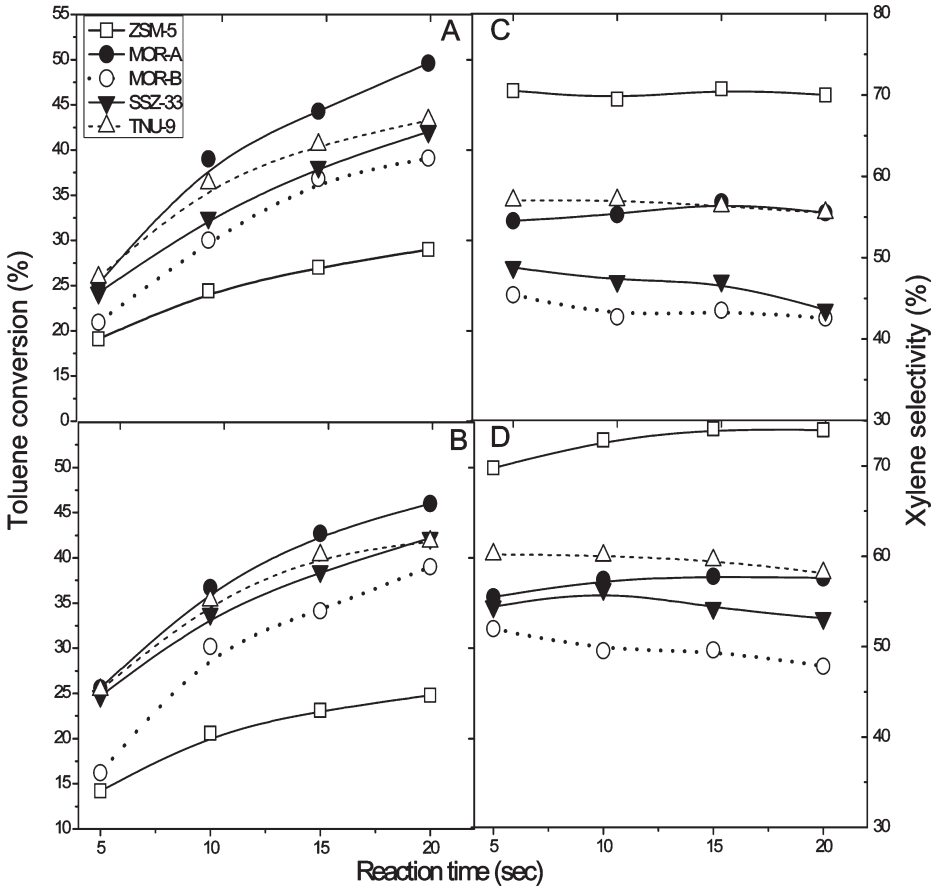

Figure 4. Reaction time dependence of toluene conversion and xylenes selectivity in toluene methylation over MOR-A (●), MOR-B (○), TNU-9 (△), SSZ-33 (▼), and ZSM-5 (□); catalyst/feed = 5, reactor = fluidized-bed, reaction temperature = 400 °C (A, C) and 350 °C (B, D).

Toluene disproportionation alone was also carried out in the fixed-bed reactor (ID 0.25 in., model # 401C-0286, Autoclave engineers) at 300, 325, 350, and 400 °C and at six different values of residence times. Figure 3 shows the effect of temperature and residence time on toluene conversion over ZSM-5 and SSZ-33 based catalyst. The result clearly indicates that conversion of toluene increases with increasing temperature and residence time. Similar to the trend noticed in toluene disproportionation in the fluidized-bed reactor, SSZ-33 based catalyst appears to be a more active catalyst for the conversion of toluene compared to ZSM-5.

3.3. Methylation of Toluene. In toluene methylation, the toluene-to-methanol molar ratio used in the feed was 1:1. The reaction was carried out at the reaction temperatures of 300, 350, and 400 °C in the fluidized-bed reactor, while the reaction was carried out in the fixed-bed reactor at reaction temperatures of 300, 325, 350, and 400 °C. Using the fluidized-bed reactor, the influence of the reaction temperature on the reaction time dependence of the conversion of toluene and the selectivities to xylenes is plotted in Figure 4 for the five zeolite catalysts investigated in the present study. Toluene conversion over all the five zeolite catalysts (ZSM-5, TNU-9, MOR-A, MOR-B, and SSZ-33) increased with reaction time and temperature, and the xylene selectivities over ZSM-5, TNU-9, MOR-A, MOR-B, and SSZ-33 were quite stable with reaction time. It was noticed that toluene conversion increases during the methylation of toluene in the following order: ZSM-5 (29.0%) < MOR-B (39.1%) < SSZ-33 (42.0%) < TNU-9 (43.3%) < MOR-A (49.6%) at 400 °C for a reaction time of 20 s. Toluene conversions do not follow the order of the channel sizes and their dimensionality. In such a case, the catalyst based on SSZ-33 should dictate. It is evident from the order of toluene conversions presented that the order of toluene conversions cannot be directly related to the increasing pore size or connectivity of individual zeolite channels.

The conversion of toluene was less than 16% when toluene alone was reacted over a catalyst based on ZSM-5 (Figure 1B). Using the same reaction conditions for toluene disproportionation alone, addition of methanol to toluene increased the conversion of toluene from 16% to 29% (Figure 4A), indicating that methylation of toluene with methanol is a faster reaction as compared with toluene disproportionation alone. In toluene methylation, the selectivity to xylenes increased to 77.7% at 300 °C as compared with the 49.7% noticed in toluene disproportionation alone and about 73.1% at 350 °C as compared with 50.0% observed in toluene disproportionation, all at reaction time of 20 s. The increase in xylene selectivities noticed in the methylation reaction is due to the nature of the methylation reaction where one mole of toluene produces one mole of xylene. Xylenes, benzene, trimethylbenzenes, and tetramethylbenzenes were the major products noticed in the methylation of toluene over MOR-A and MOR-B based catalysts (Figure 5). A maximum toluene conversion of ~49.6% was observed over MOR-A, while a maximum toluene conversion of 39.1% was noticed over MOR-B, both at 400 °C for a reaction time of 20 s (Figure 4A). This is a different scenario from what was observed in the transformation of toluene over both catalysts (MOR-A and MOR-B), in which the mordenite (MOR-B) with the higher acidity was found

dx.doi.org/10.1021/ie1018904 |*Ind. Eng. Chem. Res.* 2011, 50, 3169–3183

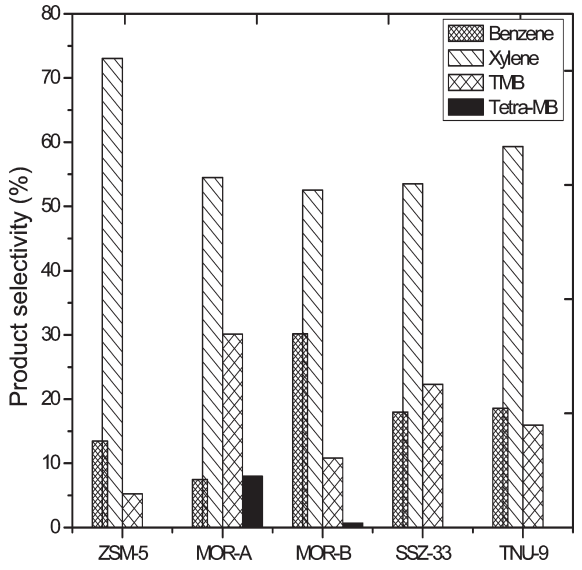

Figure 5. Product selectivity of toluene methylation over ZSM-5, SSZ-33, TNU-9 MOR-A, and MOR-B at 25% toluene conversion (toluene/methanol, 1:1 mol ratio; reactor = fluidized-bed; catalyst/feed = 5, reaction temperature: 300, 350, and 400 °C).

to be a more active catalyst in the disproportionation of toluene as compared with MOR-A, which is of a lower acidity. The selectivity toward trimethylbenzenes and xylenes showed no dependence on temperature over MOR-A, while tetramethylbenzenes and benzene showed comparable selectivity over MOR-A. On the other hand, with a decrease in temperature from 400 to 300 °C, a slight increase in xylenes, trimethylbenzenes, and tetramethylbenzenes selectivities were noticed over MOR-B, while benzene selectivity was observed to increase with temperature. Comparison between MOR-A and MOR-B at constant conversion level of ∼39% showed a significant amount of gaseous hydrocarbons over MOR-B (4.2%), as compared with ∼0.4% of gaseous hydrocarbons noticed over MOR-A. Benzene yield of ∼13.2% was noticed over MOR-B, as compared with ∼2.9% benzene yield observed over MOR-A, also at a constant toluene conversion of ∼39%. This goes to confirm a higher rate of disproportionation over MOR-B as compared with MOR-A, in the methylation of toluene with methanol. The higher rate of disproportionation noticed over MOR-B might be connected with the concentration of this zeolite based catalyst (Table 1). Toluene conversions increased with reaction time over TNU-9 and SSZ-33 based catalyst for all the temperatures studied. In the case of SSZ-33, the conversion of toluene remains largely insensitive to reaction temperature (Figure 4A,B). Benzene selectivity increased from 17.2% at 300 °C to 22.0% at 350 °C and then to 29.8% at 400 °C, while the xylene selectivity decreased from 58.0% at 300 °C to 52.3% at 350 °C and then to 43.6% at 400 °C, over SSZ-33 based catalyst at reaction time of 20 s. The reduction in xylene selectivity observed as temperature increases can be attributed to further alkylation of xylene to trimethylbenzene or can be due to toluene transalkylation with xylene to produce trimethylbenzene and benzene. Similar to the trend which was noticed over SSZ-33 based catalyst, xylene selectivity over TNU-9 based catalyst was also observed to decrease with increasing temperature. For example, at 300 °C, xylene selectivity dropped from 62.5% to 58.7% at 350 °C and then to 56.3% at 400 °C, all at a reaction time of 15 s. The decrease in xylene selectivity observed over TNU-9 can also be as a result of competitive secondary reactions.

Figure 5 summarizes the product selectivity during the methylation of toluene over ZSM-5, TNU-9, SSZ-33, MOR-A, and MOR-B at constant conversion level of 25%. The results show that xylene is obtained as the most predominant product over all the catalysts. The difference in products observed over ZSM-5, TNU-9, SSZ-33, and MOR catalysts is in agreement with the observation made by Cejka et al.[33] that the actual composition of the reaction products is strongly influenced not only by the reaction conditions applied but also by the reaction volume and the pore architecture of the particular zeolite structure. In the methylation of toluene with methanol over the different zeolite catalysts under study, the highest disproportionation rate was observed over MOR-B, since the reactivity of toluene disproportionation corresponds to the amount of benzene produced and might be connected with the concentration of this zeolite. It can be observed from Figure 5 that tetramethylbenzenes were only noticed over the mordenite based catalysts (MOR-A and MOR-B). The formation of tetramethylbenzenes in these zeolites is a result of channel intersection in mordenite that allows more reaction space for the formation of bulky intermediates and products.

The mechanism of the methylation of aromatic rings on zeolite catalysts was for the first time reported by Venuto and Landis,[34] and the analogous mechanism was presented by Kaeding et al.[35] for the methylation of toluene, whereas coadsorption of toluene and methanol on H-ZSM-5 zeolites was examined by Mirth and Lercher.[36] It is currently accepted that toluene ring alkylation with methanol proceeds via chemisorptions of methanol on the acid sites, followed by the formation of surface-active species such as methoxy groups or methoxonium ions,[37] which can further react with weakly adsorbed toluene. The elucidation of this mechanism requires a detailed knowledge of the surface species formed upon methanol and their interaction with the surface of the catalyst and the reactivity of these species during toluene methylation. It is believed that both xylenes and trimethylbenzene formed proceeded via the reaction of surface proton with methanol to form water and surface methyl cation (methoxy cation) as Scheme 1. A methyl cation attacks the toluene ring[37] carbon atom at the ortho, meta, or para position atom to form protonated xylene. Protonated xylene returns a proton to the surface and becomes xylene. Trimethylbenzenes are formed through the same mechanism, in which methyl cation (methoxy cation) attacks the xylene ring carbon atom to form a protonated trimethylbenzene. The protonated trimethylbenzene returns a proton to the surface to produce trimethylbenzene.

The results of the methylation of toluene at different reaction temperatures and residence times over ZSM-5 based catalyst using the fixed-bed reactor are presented in Table 2. The experimental results showed that methylation took place as the major reaction, while toluene disproportionation was not well pronounced at these temperatures. Similar to the trend of toluene conversion noticed in the fluidized-bed reactor in toluene methylation, the conversion of toluene increased with residence time and temperature. Xylene was obtained as the major product, while benzene and trimethylbenzenes became more significant at the higher temperatures. Similarly, the methylation of toluene was also carried out over SSZ-33 based catalyst at 300, 325, 350, and 400 °C, using the fixed-bed reactor. Xylenes and trimethylbenzenes were obtained as the major products, while a negligible amount of benzene was noticed at these temperatures as presented

Scheme 1. Possible Mechanism for Toluene Methylation

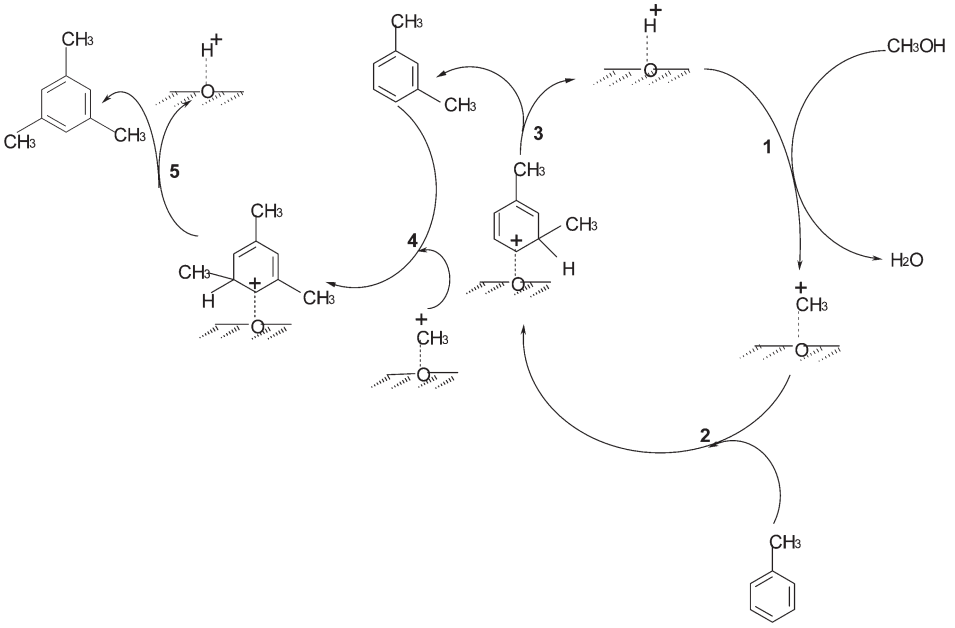

Table 2. Product Distribution (wt %) at Various Reaction Conditions for Toluene Methylation over ZSM-5 Based Catalyst Using the Fixed-Bed Reactor[a]

residence time (s)	toluene conv. (%)	gases	benzene	para xylene	meta xylene	ortho xylene	total xylene	TMBs
			Reaction Temperature = 300 °C					
0.45	0.43	0.06	0	0.09	0.17	0.02	0.28	0.08
0.54	1.10	0.12	0	0.24	0.41	0.02	0.67	0.31
0.67	1.78	0.40	0	0.33	0.52	0.13	0.98	0.40
0.90	2.64	0.42	0	0.45	0.76	0.31	1.52	0.70
1.35	4.60	0.61	0	0.88	1.71	0.41	3.00	0.99
2.70	9.90	0.73	0	2.88	3.81	0.59	7.28	1.90
			Reaction Temperature = 325 °C					
0.43	2.43	0.15	0	0.59	1.06	0.29	1.94	0.34
0.51	4.00	0.19	0	0.71	1.39	0.34	2.44	1.37
0.64	5.10	0.80	0	0.74	1.75	0.43	2.92	1.66
0.86	8.23	0.99	0	1.66	2.57	0.85	5.08	2.16
1.29	10.38	1.31	0.19	2.37	2.82	0.91	6.10	2.78
2.59	15.60	1.67	0.22	4.33	5.15	1.11	10.59	3.11

[a] T = 300 and 325 °C; toluene/methanol, 1:1 mol ratio; catalyst loading, 400 mg.

in Table 3. Using the fixed-bed reactor, the toluene conversion and xylene selectivity are illustrated in Figure 6. The conversion of toluene increased with residence time and temperature over SSZ-33 and ZSM-5 and attains a maximum of 46.2% and 31.0%, respectively, at 400 °C. Similar to the xylene selectivity observed in the fluidized-bed reactor, catalyst based on ZSM-5 showed a higher selectivity toward xylene as compared to its selectivity over SSZ-33 based catalyst. At all temperatures studied, the selectivity to xylenes for SSZ-33 was lower than that obtained over ZSM-5 (Figure 6C,D), which indicates that other reactions (xylene methylation and xylene transalkylation) besides toluene methylation proceed to a greater extent inside the channels of SSZ-33, as compared to ZSM-5 based catalyst.

All the three isomers of xylene were detected in the GC analysis of the reaction product. Comparing the p/o ratios over ZSM-5, TNU-9, SSZ-33, MOR-A, and MOR-B at a constant conversion level of 25%, the p/o ratio was found to be between the range of ∼1.1 and ∼1.6, when the fluidized-bed reactor was used. Similarly, the p/o ratio was also compared over ZSM-5 and SSZ-33 at a constant conversion level of ∼8%, when the fixed-bed reactor was used. The p/o ratio was noticed to be between the range of ∼1.1 (SSZ-33) and ∼2.0 (ZSM-5). It is clear from the results of p/o ratios presented that, for all the zeolite based catalysts studied, p/o was found to be higher than the equilibrium value, which was reported by Kaeding et al.[35] to be approximately 0.9 between 350 and 600 °C. The p/o ratio noticed over SSZ-33 based catalyst was found to be close to the equilibrium value obtained by Kaeding et al.[35] It was recently reported that zeolite SSZ-33 shows catalytic behavior closer to large pore zeolites such as beta, than to ZSM-5.[13]

dx.doi.org/10.1021/ie1018904 |*Ind. Eng. Chem. Res.* 2011, 50, 3169–3183

Table 3. Product Distribution (wt %) at Various Reaction Conditions for Toluene Methylation over SSZ-33 Based Catalyst Using the Fixed-Bed Reactor[a]

residence time (s)	toluene conv. (%)	gases	benzene	para xylene	meta xylene	ortho xylene	total xylene	TMBs
			Reaction temperature = 300 °C					
0.45	4.73	0.61	0	0.43	1.20	0.41	2.05	2.04
0.54	7.84	0.83	0	0.83	2.56	0.75	4.16	2.85
0.67	9.23	0.90	0	0.85	2.67	0.76	4.29	4.04
0.90	14.12	0.92	0	1.64	4.41	1.49	7.54	5.71
1.35	17.88	1.00	0.22	2.33	5.31	2.01	9.25	7.01
2.70	19.32	1.37	0.23	2.41	5.41	2.38	10.20	7.52
			Reaction temperature = 325 °C					
0.43	12.93	0.83	0	1.35	4.08	1.28	6.72	5.38
0.51	18.50	1.50	0	2.09	5.14	2.01	9.24	7.76
0.64	20.40	1.71	0	2.06	5.81	2.01	9.88	8.81
0.86	22.00	2.02	0	2.23	5.70	2.10	10.03	9.95
1.29	24.44	2.07	0.54	2.56	6.37	2.23	11.16	10.67
2.59	27.64	2.21	0.58	3.71	6.33	3.14	13.18	11.67

[a] T = 300 and 325 °C; toluene/methanol, 1:1 mol ratio; catalyst loading, 400 mg.

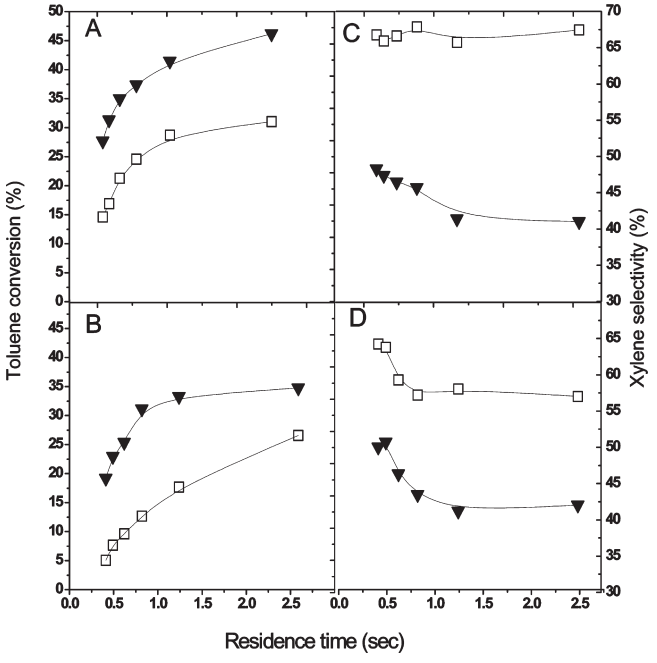

Figure 6. Residence time dependence of toluene conversion and xylenes selectivity in toluene methylation over SSZ-33 (▼) and ZSM-5 (□); reactor = fixed-bed, reaction temperature = 400 °C (A, C) and 350 °C (B, D).

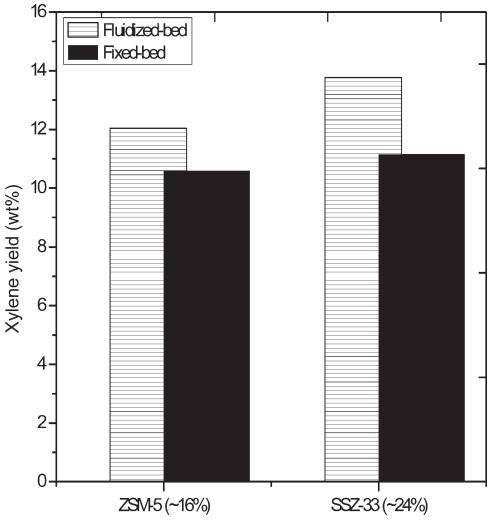

Figure 7. Xylene yield in toluene methylation over ZSM-5 and SSZ-33 at constant conversion level of 16% and 24%, respectively, using fixed-bed (■) and fluidized-bed (striped square) reactors (reaction temperatures: 300, 325, and 350 °C).

3.4. Comparison of Disproportionation and Methylation Reactions in Fluidized and Fixed-Bed Reactors. Some researchers have preferred the fluidized-bed reactor as an attractive option to the fixed-bed reactor for some reactions. This is because the fluidized-bed reactor provides a high rate of heat transfer in order to maintain the isothermal operation[38] and also because of catalyst fluidization. Generally, the difference between the fluidized-bed and the fixed-bed reactors is caused mainly by heat transfer effects.[39] Toluene disproportionation and methylation reactions were successfully investigated in fixed and fluidized-bed reactors. Comparison between the xylene yield in toluene methylation over ZSM-5 and SSZ-33 at constant conversion level of 16% and 24%, respectively, using both the fluidized and fixed-bed reactors was also investigated. Figure 7 shows the xylene yield over two different zeolite based catalysts in two different reactors. In the methylation reaction, the fluidized-bed reactor showed a slightly higher xylene yield than the yield noticed in the fixed-bed reactor over both zeolite catalysts. Figure 8 shows the para-xylene selectivity in toluene methylation over the zeolite based catalysts using fluidized- and fixed-bed reactors at constant conversion level of 25% and 5%, respectively. In both the fluidized- and fixed-bed reactors, the medium pore zeolites (ZSM-5 and TNU-9) showed higher para selectivity as compared with the large pore zeolites. This result is consistent with the observation made by Raj et al.[40] that medium pore zeolites exhibiting channels with dimensions of about 0.55 nm have led to shape selectivity in the processing of alkyl aromatics,

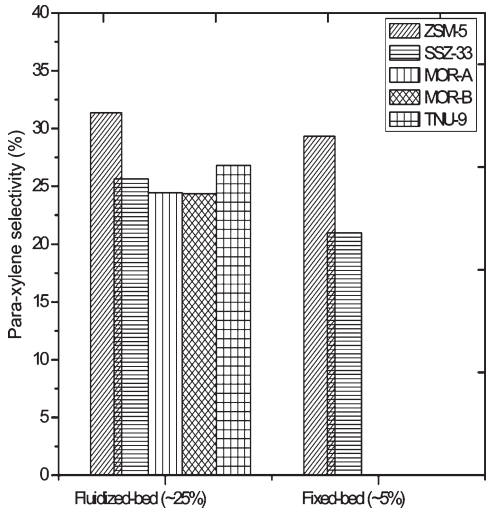

Figure 8. Para-xylene selectivity in toluene methylation over zeolite based catalysts using fixed-bed and fluidized-bed reactors at constant conversion level of 5% and 25%, respectively; reaction temperature: 300, 350, and 400 °C.

Scheme 2

$$2T \underset{k_{-x1}}{\overset{k_{x1}}{\rightleftharpoons}} \text{Dispro. Products}\ [\text{Xylenes + Benzene}]$$

particularly with respect to para isomers of dialkyl aromatic hydrocarbons.

4. KINETIC MODELING

4.1. Model Formulation. Developing a comprehensive universal kinetic model which illustrates the reaction of toluene with methanol over all the zeolite based catalysts under study is the main objective of this section. Therefore, two kinetic schemes have been studied. The first scheme (Scheme 2) represents the disproportionation of toluene to give xylenes and benzene. The other scheme (Scheme 3) represents the overall reaction involving disproportionation and methylation. It should be noted that the following assumptions were made in deriving the reaction network: (1) The disproportionation of toluene follows second order kinetics, and a reversible reaction path is assumed for the disproportionation reaction.[41,42]. (2) For the reactions in the fluidized-bed reactor, catalysts deactivation is assumed to be a function of time-on-stream (TOS). (3) Isothermal operating conditions can also be assumed given the design of the riser simulator unit and the relatively small amount of reacting species.[29] Furthermore, isothermal operation was assumed for reactions in the fixed-bed reactor, as no change in the temperature was observed during the course of the reaction. (4) A single effectiveness factor was considered for toluene, xylene, trimethylbenzene, and tetramethylbenzene. (5) The effectiveness factor η was taken to be unity. This assumption was made based on the fact that p-xylene formed by catalytic reaction can easily escape via the pores of ZSM-5[43] comparing mordenite with a larger pore opening; no diffusion restriction is expected in this reaction. (6) For the reactions in the fixed-bed reactor, it was assumed that the catalysts do not deactivate, since it was observed experimentally that the catalysts did not deactivate during the course of the reaction due to high H_2 pressure. Furthermore, Comelli et al.[44] showed that, at high hydrogen pressure, coke formation was almost negligible and, thus, the activity of the catalyst was not lost.

4.1.1. Model I: Disproportionation of Toluene. To develop a suitable kinetic model representing the transformation of toluene, the reaction network shown in Scheme 2 is used.

For toluene disproportionation in the fluidized-bed reactor, the following set of species balances and catalytic reactions can be written.

Rate of disappearance of toluene

$$\frac{dy_T}{dt} = -\left(2\eta A_1 k_{X1} {y_T}^2 - \eta A_2 \frac{k_{X1}}{K_{eq}} y_B y_{XY}\right)\frac{W_c}{V}\exp(-\alpha t) \quad (1)$$

Rate of formation of disproportionation products

$$\frac{dy_{disp}}{dt} = \left(\eta A_3 k_{X1} {y_T}^2 - \eta A_4 \frac{k_{X1}}{K_{eq}} y_B y_{XY}\right)\frac{W_c}{V}\exp(-\alpha t) \quad (2)$$

where y_x is the mass fraction of species x in the riser simulator, W_{hc} is the weight of feedstock injected into the reactor (0.162 g), MW_x is the molecular weight of specie x in the system, V is the volume of the riser (45 cm^3), W_C is the mass of the catalyst (0.81 g of catalyst), t is the time (s), η = an effectiveness factor, and k is the rate constant (cm^3/(g of catalyst·s)). Also, A_1, A_2, A_3, and A_4 are lumped constants given below.

$$A_1 = \frac{W_{hc}}{VMW_T} \quad A_2 = \frac{W_{hc}MW_T}{VMW_BMW_{XY}}$$

$$A_3 = \frac{W_{hc}MW_{dispro(avg)}}{VMW_T{}^2} \quad A_4 = \frac{W_{hc}MW_{dispro(avg)}}{VMW_BMW_{XY}}$$

In order to ensure thermodynamic consistency at equilibrium, the rate constants for toluene to the disproportionation products (benzene + xylene) in the above equations are expressed as follows:

$$k_{-x1} = \frac{k_{x1}}{K_{eq}}$$

where K_{eq} is a temperature-dependent equilibrium constant. The equilibrium constant (K_{eq}) is obtained from a published work.[41]

Similarly, for toluene disproportionation in the fixed-bed reactor, the following set of species balances and catalytic reactions can be written.

Rate of disappearance of toluene

$$\frac{dy_T}{dt_\tau} = -\left(2\eta F_1 k_{X1} {y_T}^2 - \eta F_2 \frac{k_{X1}}{K_{eq}} y_B y_{XY}\right) \quad (3)$$

Rate of formation of disproportionation products

$$\frac{dy_{disp}}{dt_\tau} = \eta F_3 k_{X1} {y_T}^2 - \eta F_4 \frac{k_{X1}}{K_{eq}} y_B y_{XY} \quad (4)$$

where t_τ is the reaction time, at inlet of the catalyst bed $t_\tau = 0$ and at the oulet of the catalyst bed, $t_\tau = \tau$. F_{TM} is the total mass flow rate, MW_x is the molecular weight of specie x in the system, and

dx.doi.org/10.1021/ie1018904 |Ind. Eng. Chem. Res. 2011, 50, 3169–3183

Scheme 3

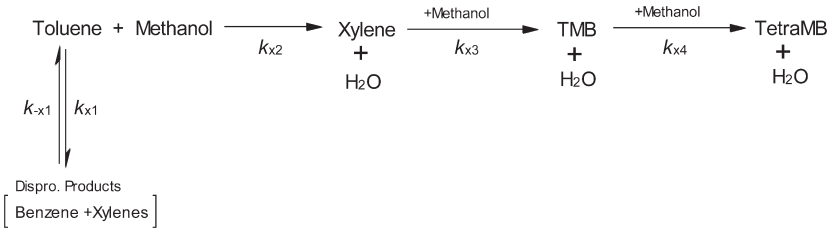

v_o is the total volumetric flow rate where F_1, F_2, F_3, and F_4 are lumped constants given below.

$$F_1 = \frac{F_{TM}}{v_o MW_T} \quad F_2 = \frac{F_{TM} MW_T}{v_o MW_B MW_{XY}}$$

$$F_3 = \frac{F_{TM} MW_{dispro(avg)}}{v_0 {MW_T}^2} \quad F_4 = \frac{F_{TM} MW_{dispro(avg)}}{v_0 MW_B MW_{XY}}$$

The temperature dependence of the rate constants was represented with the centered temperature form of the Arrhenius equation, i.e.,

$$k_i = k_{oi} \exp\left[\frac{-E_i}{R}\left(\frac{1}{T} - \frac{1}{T_o}\right)\right] \tag{5}$$

where T_o is an average temperature introduced to reduce parameter interaction,[45] k_{oi} is the rate constant for reaction i at T_o, and E_i is the activation energy for reaction i.

4.1.2. Model II: Methylation of Toluene with Methanol. In this section, a comprehensive universal kinetic model for toluene methylation over all the zeolite based catalysts under study was developed. To develop a suitable kinetic model representing the overall methylation of toluene with methanol, we propose the reaction network shown in Scheme 3.

4.1.3. Model Development for Toluene Methylation over Zeolite Based Catalysts Using a Fluidized-Bed Reactor. On the basis of the product distribution observed in the methylation reaction over all zeolite based catalysts under study, a suitable kinetic model representing the methylation reaction can be developed. The following set of species balances and catalytic reactions can be written.

Rate of disappearance of toluene

$$\frac{dy_T}{dt} = -\left(2\eta A_1 k_{X1} {y_T}^2 + \eta A_2 k_{X2} y_T y_M - \eta A_3 \frac{k_{X1}}{K_{eq}} y_B y_{XY}\right)\frac{W_c}{V} \exp(-\alpha t) \tag{6}$$

Rate of formation of xylene

$$\frac{dy_{XY}}{dt} = (\eta A_4 k_{X2} y_T y_M - \eta A_2 k_{X3} y_{XY} y_M)\frac{W_c}{V} \exp(-\alpha t) \tag{7}$$

Rate of formation of trimethylbenzene

$$\frac{dy_{TMB}}{dt} = (\eta A_5 k_{X3} y_{XY} y_M - \eta A_2 k_{X4} y_{TMB} y_M)\frac{W_c}{V} \exp(-\alpha t) \tag{8}$$

Rate of formation of tetramethylbenzene

$$\frac{dy_{TetraMB}}{dt} = \eta A_6 k_{X4} y_{TMB} y_M \frac{W_c}{V} \exp(-\alpha t) \tag{9}$$

Rate of formation of disproportionation products

$$\frac{dy_{disp}}{dt} = \left(\eta A_7 k_{X1} {y_T}^2 - \eta A_8 \frac{k_{X1}}{K_{eq}} y_B y_{XY}\right)\frac{W_c}{V} \exp(-\alpha t) \tag{10}$$

where A_1, A_2, A_3, A_4, A_5, A_6, A_7, and A_8 are lumped constants given below.

$$A_1 = \frac{W_{hc}}{VMW_T} \quad A_2 = \frac{W_{hc}}{VMW_M} \quad A_3 = \frac{W_{hc} MW_T}{VMW_B MW_{XY}}$$

$$A_4 = \frac{W_{hc} MW_{XY}}{VMW_T MW_M}$$

$$A_5 = \frac{W_{hc} MW_{TMB}}{VMW_{XY} MW_M} \quad A_6 = \frac{W_{hc} MW_{TetraMB}}{VMW_{TMB} MW_M}$$

$$A_7 = \frac{W_{hc} MW_{dispro(avg)}}{VMW_T{}^2} \quad A_8 = \frac{W_{hc} MW_{dispro(avg)}}{VMW_B MW_{XY}}$$

Kinetic model development for toluene methylation over ZSM-5, SSZ-33, TNU-9, and mordenite was developed on the basis of Scheme 3. In toluene methylation, tetramethylbenzene is one of the major products noticed over mordenite based catalysts (MOR-A and MOR-B), but in the case of ZSM-5, SSZ-33, and TNU-9, $k_{X4} \approx 0$, due to absence of TetraMB. Also, k_{X4} was assumed to be equal to zero over MOR-B, since the maximum amount of tetramethylbenzenes noticed over MOR-B (~0.2%) was very small.

4.1.4. Model Development for Toluene Methylation over SSZ-33 and ZSM-5 Based Catalysts Using a Fixed-Bed Reactor. On the basis of the products distribution noticed in the methylation reaction over SSZ-33 and ZSM-5 using the fixed-bed reactor, a suitable kinetic model based in Scheme 3 was also developed.

Rate of disappearance of toluene

$$\frac{dy_T}{dt_\tau} = -\left(2\eta G_1 k_{X1} {y_T}^2 + \eta G_2 k_{X2} y_T y_M - \eta G_3 \frac{k_{X1}}{K_{eq}} y_B y_{XY}\right) \tag{11}$$

Rate of formation of xylene

$$\frac{dy_{XY}}{dt_\tau} = \eta G_4 k_{X2} y_T y_M - \eta G_2 k_{X3} y_{XY} y_M \tag{12}$$

dx.doi.org/10.1021/ie1018904 |*Ind. Eng. Chem. Res.* 2011, 50, 3169–3183

Table 4. Estimated Kinetic Parameters for Toluene Transformation over Mordenite, ZSM-5, SSZ-33, and TNU-9 Based on Time-on-Stream (TOS) Using the Fluidized-Bed Reactor[a]

MOR-A	MOR-B	ZSM-5	SSZ-33	TNU-9
$E_{M1\text{-}A}$	$E_{M1\text{-}B}$	E_{Z1}	E_{S1}	$E_{TNU\text{-}1}$
50.4 ± 5.2	16.2 ± 2.2	47.0 ± 4.8	14.9 ± 1.6	17.1 ± 1.5
$k_{M1O\text{-}A} \times 10^4$	$k_{M1O-B} \times 10^4$	$k_{Z1O} \times 10^4$	$k_{S1O} \times 10^4$	$k_{TNU\text{-}1O} \times 10^4$
0.097 ± 0.013	0.398 ± 0.024	0.571 ± 0.009	0.263 ± 0.012	0.451 ± 0.021
α (1/s)	α (1/s)	α (1/s)	α (1/s)	α (1/s)
0.050 ± 0.004	0.053 ± 0.007	0.043 ± 0.014	0.071 ± 0.008	0.051 ± 0.009

[a] k_i (m^6/kg of catalyst·s); E_i (kJ/mol).

Table 5. Estimated Kinetic Parameters for Toluene Transformation over ZSM-5 and SSZ-33 Using the Fixed-Bed Reactor[a]

ZSM-5	SSZ-33
E_{Z1}	E_{S1}
88.1 ± 4.2	67.5 ± 5.0
$k_{Z1O} \times 10^4$	$k_{S1O} \times 10^4$
0.483 ± 0.031	0.495 ± 0.040

[a] k_i (s^{-1}); E_i (kJ/mol).

Table 6. Estimated Kinetic Parameters for the Methylation of Toluene over Mordenite and ZSM-5 Based on TOS Model Using the Fluidized-Bed Reactor[a]

MOR-A			ZSM-5	
$E_{M2\text{-}A}$	$E_{M3\text{-}A}$	$E_{M4\text{-}A}$	E_{Z2}	E_{Z3}
13.1 ± 2.2	10.1 ± 3.9	54.5 ± 16.2	46.8 ± 3.1	39.7 ± 10.1
$k_{M2O\text{-}A} \times 10^4$	$k_{M3O\text{-}A} \times 10^4$	$k_{M4O\text{-}A} \times 10^4$	$k_{Z2O} \times 10^4$	$k_{Z3O} \times 10^4$
1.183 ± 0.009	0.572 ± 0.151	0.787 ± 0.065	1.733 ± 0.002	0.883 ± 0.012
α (1/s)			α (1/s)	
0.039 ± 0.001			0.030 ± 0.006	
MOR-B				
$E_{M2\text{-}B}$				$E_{M3\text{-}B}$
13.9 ± 3.6				13.2 ± 3.1
$k_{M2O-B} \times 10^4$				$k_{M3O-B} \times 10^4$
0.663 ± 0.167				0.924 ± 0.118
α (1/s)				
0.049 ± 0.003				

[a] k_i (m^6/kg of catalyst·s); E_i (kJ/mol).

Rate of formation of trimethylbenzene

$$\frac{dy_{TMB}}{dt_\tau} = \eta G_5 k_{X3} y_{XY} y_M \qquad (13)$$

Rate of formation of disproportionation products

$$\frac{dy_{disp}}{dt_\tau} = \eta G_6 k_{X1} {y_T}^2 - \eta G_7 \frac{k_{X1}}{K_{eq}} y_B y_{XY} \qquad (14)$$

where G_1, G_2, G_3, G_4, G_5, G_6, and G_7 are lumped constants given below.

$$G_1 = \frac{F_{TM}}{v_o MW_T} \quad G_2 = \frac{F_{TM}}{v_o MW_M}$$

$$G_3 = \frac{F_{TM} MW_T}{v_o MW_B MW_{XY}} \quad G_4 = \frac{F_{TM} MW_{XY}}{v_0 MW_T MW_M}$$

$$G_5 = \frac{F_{TM} MW_{TMB}}{v_0 MW_{XY} MW_M} \quad G_6 = \frac{F_{TM} MW_{dispro(avg)}}{v_0 {MW_T}^2}$$

$$G_7 = \frac{F_{TM} MW_{dispro(avg)}}{v_0 MW_B MW_{XY}}$$

4.2. Discussion of Kinetic Modeling Results. The kinetic parameter values determined (k_{oi}, E_i, α) for the methylation reaction were obtained using nonlinear regression (MATLAB package). It can be observed that the parameters of model I are subsets of the parameters belonging to the comprehensive model (model II). It was, therefore, decided to fit models I first and then use the calculated values from this model in model II. This approach was implemented in order to reduce correlation between kinetic parameters in the comprehensive model. The values of the model parameters along with their corresponding 95% confidence limits (CLs) are shown in Tables 4, 5, 6, 8 and 10, while the resulting cross-correlation matrices are also given in Table 7 for ZSM-5 and Table 9for TNU-9 based catalyst. It can be observed from the tabulated results that the apparent activation energy for the disproportionation of toluene over MOR-A, MOR-B, ZSM-5, SSZ-33, and TNU-9 were 50.4 ± 5.2, 16.2 ± 2.2, 47.0 ± 4.8, 14.9 ± 1.6, and 17.1 ± 1.5, respectively, for the fluidized-bed reactor, while 88.1 ± 4.2 and 67.5 ± 5.0 were obtained over ZSM-5 and SSZ-33, respectively, for the fixed-bed reactor. Bhavikatti and Patwardhan[41] reported an apparent energy of actiavtion of ~60.7 kJ/mol over the Ni/mordenite, while ~54.3 kJ/mol was reported by Chang et al.[46] for the same reaction over a commercial solid catalyst. These values are in agreement or have the same order with the values of the apparent energies of activation observed over mordenite and ZSM-5 based catalyst (50.4 and 47.0 kJ/mol) in the present study despite our differences in conversion.

dx.doi.org/10.1021/ie1018904 |Ind. Eng. Chem. Res. 2011, 50, 3169–3183

Table 7. Correlation Matrix for Toluene Methylation over ZSM-5 Based Catalyst Using the Fluidized-Bed Reactor

	k_{Z1}	E_{Z1}	α	k_{Z2}	E_{Z2}	α	k_{Z3}	E_{Z3}	α
$k_{Z1,2,3}$	1.0000	−0.3566	0.8671	1.0000	−0.7203	0.8196	1.0000	−0.6459	0.5934
$E_{Z1,2,3}$	−0.3566	1.0000	−0.1848	−0.7203	1.0000	−0.3794	−0.6459	1.0000	0.0111
α	0.8671	−0.1848	1.0000	0.8196	−0.3794	1.0000	0.5934	0.0111	1.0000

Table 8. Estimated Kinetic Parameters for the Methylation of Toluene over SSZ-33 and TNU-9 Based on TOS Model Using the Fluidized-Bed Reactor[a]

SSZ-33		TNU-9	
E_{S2}	E_{S3}	$E_{TNU\text{-}2}$	$E_{TNU\text{-}3}$
8.2 ± 2.2	7.1 ± 1.1	33.9 ± 3.3	32.1 ± 1.2
$k_{S2O} \times 10^4$	$k_{S3O} \times 10^4$	$k_{TNU\text{-}2O} \times 10^4$	$k_{TNU\text{-}3O} \times 10^4$
1.459 ± 0.189	2.161 ± 0.043	1.375 ± 0.148	1.388 ± 0.092
α (1/s)		α (1/s)	
0.050 ± 0.012		0.025 ± 0.007	

[a] k_i (m^6/kg of catalyst·s); E_i (kJ/mol).

Table 4 presents the apparent energies of activation over the two mordenite based catalysts used in this study. It was noticed that the apparent activation energy for the disproportionation of toluene over MOR-A (50.4 kJ/mol) is higher than the 16.2 kJ/mol obtained in toluene disproportionation over MOR-B based catalyst. Since both catalysts are based on the same zeolite, the issue of diffusional limitation is not probably the major contributing factor in explaining the difference in apparent energies of activation noticed over both catalysts. It is a well established fact that the intrinsic activation energy is a function of catalyst acidity. Catalysts of high acidity lead to low intrinsic activation energy. As presented in Table 1, MOR-B is approximately three times more acidic than MOR-A, which is almost likely to lead to a lower intrinsic activation energy of toluene over MOR-B, as compared with MOR-A. According to Levenspiel,[47] the apparent activation energy is equivalent to half of the summation of the intrinsic activation energy and the diffusion activation energy. Therefore, on the basis of the low intrinsic activation energy over MOR-B, a lower apparent energy of activation is expected over MOR-B, as comapred with MOR-A. It can be observed from Table 4 that the apparent activation energy for the disproportionation of toluene over TNU-9 is lower as compared with the value noticed over ZSM-5 based catalyst (47.0 kJ/mol). Although both ZSM-5 and TNU-9 are three-dimensional zeolite with 10-ring channel systems, the size of the channels of TNU-9 is 0.52 nm × 0.60 nm and 0.51 nm × 0.55 nm, thus slightly larger zeolite compared with ZSM-5. Therefore, the activation energy for toluene diffusion (E_D) over ZSM-5 based catalyst is greater than the E_D in TNU-9 based catalyst. E_D (ZSM-5) > E_D (TNU-9); therefore, the apparent activation energy for toluene disproportionation over ZSM-5 ($E_{app\text{-}ZSM\text{-}5}$) is greater than the apparent activation energy for toluene disproportionation over TNU-9 catalyst ($E_{app\text{-}TNU\text{-}9}$).

On the other hand, apparent activation energies of 88.1 and 67.5 kJ/mol were obtained for toluene disproportionation over ZSM-5 and SSZ-33 based catalyst, respectively, when a fixed-bed reactor was used. The higher apparent activation energy for toluene disproportionation noticed over ZSM-5 based catalyst as compared with SSZ-33 is as a result of the high activation energy for toluene diffusion (E_D) over ZSM-5, due to its pore opening and pore geometry. It has been generally observed from previous studies[48,49] that a lower apparent energy of activation was observed when a fluidized-bed reactor is used as compared with a fixed-bed reactor. Similar observation was also noticed during the transformation of 1,2,4-trimethylbenzene, in which Ko and Kuo[50] obtained apparent energies of activation of 37.4 and 46.6 kJ/mol for isomerization of 1,2,4-TMB to form 1,2,3-TMB and 1,3,5-TMB, respectively, as compared with an apparent energy of activation of 10.01 kJ/mol obtained by another researcher[51] for the same isomerization reaction when performed in a fluidized-bed reactor. Also, the problem of temperature and concentration gradients, which are known to adversely affect the values of estimated kinetic parameters, is greatly minimized in the fluidized-bed reactor because of intense mixing inside the reactor. On the basis of the correlation matrices of the regression analysis presented in Table 7 for methylation of toluene over ZSM-5 based catalyst, it shows the very low correlations between k_{Z1}-k_{Z3} and E_{Z1}-E_{Z3} and E_{Z1}-E_{Z3} and α and the moderate correlation between k_{Z1}-k_{Z3} and α. Similarly, Table 9 reports the very low correlations between $k_{TNU\text{-}1}$-$k_{TNU\text{-}3}$ and $E_{TNU\text{-}1}$-$E_{TNU\text{-}3}$ and $E_{TNU\text{-}1}$-$E_{TNU\text{-}3}$ and α. It can be observed that in the cross-correlation matrices presented in this study, most of the coefficients remain in the low level with only a few exceptions.

From the values of the activation energies for toluene methylation presented in Tables 6, 8, and 10 over all the zeolite based catalysts under study, it can be observed that the apparent energies of activation for methylation of toluene is in the range of 8.2−89.2 kJ/mol. Mantha et al.[52] reported an apparent activation energy of 79.8 kJ/mol for toluene methylation over ZSM-5 based catalyst, while Bhat et al.[53] reported a value of 60.5 kJ/mol over ZSM-8 based catalyst. It was reported by Mirth and Lercher[54] during their study on the coadsorption of toluene and methanol on H-ZSM-5 zeolites that the majority of the kinetic studies of toluene methylation have reported activation energies of between 50 and 90 kJ/mol. Using the fluidized-bed reactor, the apparent activation energies for toluene methylation follows the order: ZSM-5 (46.8 kJ/mol) > TNU-9 (33.9 kJ/mol) > MOR-B (13.9 kJ/mol) ≈ MOR-A (13.1 kJ/mol) > SSZ-33 (8.2 kJ/mol). Considering SSZ-33 based catalyst, which contains 12- and 10-ring interconnected channels, lower apparent activation energy for toluene methylation is expected, as compared with the medium pore ZSM-5 and TNU-9 based catalyst. The low value of apparent activation energy for toluene methylation observed over SSZ-33 may also be attributed to the reduced mass transfer resistance due to the relative larger pore size of SSZ-33 as compared with other zeolite based catalysts.

The values of apparent activation energies reported in Tables 6 and 8 show that, on mordenite catalysts, the methylation of xylene to trimethylbenzene ($E_{M3\text{-}A}$ = 10.1 kJ/mol and $E_{M3\text{-}B}$ = 13.2 kJ/mol) is easier than the methylation of xylene to trimethylbenzene over the medium pore zeolites (ZSM-5 (39.7 kJ/mol) and TNU-9 (32.1 kJ/mol)). The presence of channel

Table 9. Correlation Matrix for Toluene Methylation over TNU-9 Based Catalyst

	$k_{TNU\text{-}1}$	$E_{TNU\text{-}1}$	α	$k_{TNU\text{-}2}$	$E_{TNU\text{-}2}$	α	$k_{TNU\text{-}3}$	$E_{TNU\text{-}3}$	α
$k_{TNU1,2,3}$	1.0000	−0.0736	0.8652	1.0000	0.0185	0.8217	1.0000	−0.0115	0.7628
$E_{TNU1,2,3}$	−0.0736	1.0000	−0.5985	0.0185	1.0000	−0.0216	−0.0115	1.0000	−0.0078
α	0.8652	−0.5985	1.0000	0.8217	−0.0216	1.0000	0.7628	- 0.0078	1.0000

Table 10. Estimated Kinetic Parameters for the Methylation of Toluene over ZSM-5 and SSZ-33 Using the Fixed-Bed Reactor[a]

ZSM-5		SSZ-33	
E_{Z2}	E_{Z3}	E_{S2}	E_{S3}
89.2 ± 3.7	34.0 ± 6.1	59.9 ± 4.9	32.8 ± 7.8
$k_{Z2O} \times 10^4$	$k_{Z3O} \times 10^4$	$k_{S2O} \times 10^4$	$k_{S3O} \times 10^4$
0.263 ± 0.012	0.675 ± 0.114	0.403 ± 0.023	1.289 ± 0.126

[a] k_i (s^{-1}); E_i (kJ/mol).

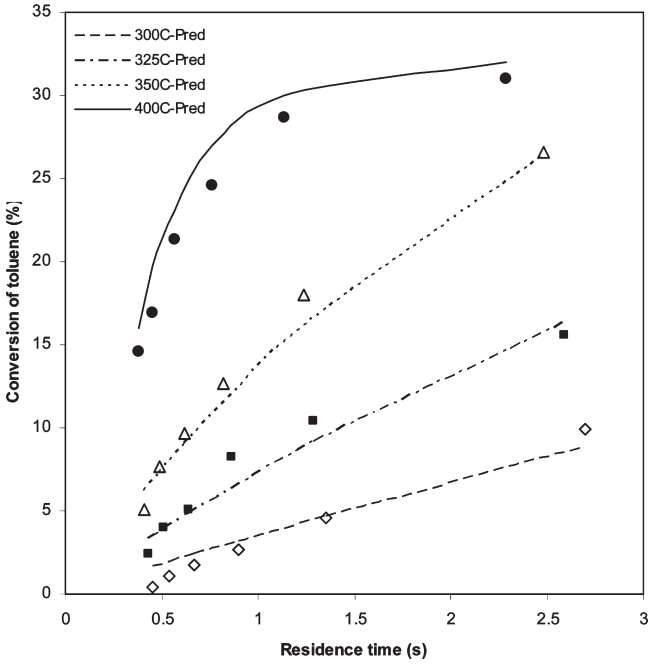

Figure 9. Comparison between experimental results and model predictions (Scheme 3) for toluene conversion in toluene methylation over ZSM-5 in the fixed-bed reactor at reaction temperature of 300 °C (◊), 325 °C (■), 350 °C (Δ), and 400 °C (●).

intersection in mordenite allows it to accommodate higher concentrations of bulky trimethylbenzene molecules inside its channel system. Also, the differences in pore size between mordenite and the medium pore zeolites accounts for this important difference in activation energies, while ZSM-5 is a medium pore zeolite containing two types of intersecting channels, near circular (0.53−0.56 nm) zigzag channels and elliptical (0.51−0.55 nm) straight chain channels, TNU-9 with 0.52 × 0.60 nm and 0.51 × 0.55 nm and mordenite, a one-dimensional large pore zeolite with a nominal free diameter of 0.67−0.70 nm. Trimethylbenzene molecule would pass through the pores of mordenite without much hindrance even though the channel diameter of the zeolite is smaller than the critical size of trimethylbenzene molecule. It is of paramount importance to note that molecules are not rigid bodies and neither are the zeolites. Both molecules and windows vibrate, and mutual distortion of the two occurs when molecules penetrate through the zeolite framework.[55] It is important to note the difference between the apparent energies of activation for toluene methylation (MOR-B 13.9 kJ/mol, MOR-A 13.1 kJ/mol, ZSM-5 46.8 kJ/mol, SSZ-33 8.2 kJ/mol, TNU-9 33.9 kJ/mol) and xylene methylation (MOR-B 13.2 kJ/mol, MOR-A 10.1 kJ/mol, ZSM-5 39.7 kJ/mol, SSZ-33 7.1 kJ/mol, TNU-9 32.1 kJ/mol) to form trimethylbenzene over all the zeolite based catalysts under study. The difference in the activation energies for the two reactions may be a clue that the benzene ring of aromatic compounds becomes more reactive as the number of attached methyl groups increases, so xylene reacts more easily with methanol. A graphical comparison between experimental and model predictions for ZSM-5 based catalyst is shown in Figure 9. It can be seen that the model predictions compared very well with the experimental data.

5. CONCLUSIONS

Four different structural types of zeolites (ZSM-5, TNU-9, SSZ-33, and mordenite) were investigated in disproportionation and methylation of toluene with methanol. The following conclusions can be drawn from the reactions: (1) The conversion of toluene in the methylation and disproportionation reaction follow neither the amount of acid sites of the zeolite based catalysts studied nor the increasing size and connectivity of their channels. (2) An increase in the concentration of Lewis acid sites was observed after modification of parent zeolites with alumina binder and a simultaneous decrease in the Si/Al ratio for all catalysts was noticed. (3) Xylene was obtained as the major product over all the zeolite based catalysts in the methylation of toluene with methanol. (4) In toluene disproportionation, the selectivity to the sum of xylenes over the different zeolite catalysts under study, follow the order: MOR-B < SSZ-33 < TNU-9 < ZSM-5 ≈ MOR-A. (5) The order of xylene/benzene molar ratios in toluene disproportionation indicates the increasing reaction volume provided by individual zeolites with the exception of mordenite. (6) In toluene methylation, the presence of channel intersections in mordenite based catalyst allows more reaction space for the formation of bulky intermediates and/or products. (7) In toluene methylation, the higher the toluene conversion, the higher was also the rate of competitive and consecutive reactions. (8) Using the fluidized-bed reactor, the kinetic parameters for toluene methylation were estimated by nonlinear regression analysis. The apparent activation energies were found in this order: ZSM-5 (46.8 kJ/mol) > TNU-9 (33.9 kJ/mol) > MOR-B (13.9 kJ/mol) ≈ MOR-A (13.1 kJ/mol) > SSZ-33 (8.2 kJ/mol).

■ AUTHOR INFORMATION

Corresponding Author

*Tel.: +966-3-860-1429. Fax: +966-3- 860-4234. E-mail: skhattaf@kfupm.edu.sa.

■ ACKNOWLEDGMENT

The authors acknowledge the financial support provided by King AbdulAziz City for Science and Technology for this research under the Refining and Petrochemicals Program of the National Science and Technology Plan (NSTP) for the year 2009 (09-PETE86-4). We are grateful for the support from Ministry of Higher Education, Saudi Arabia, for the establishment of the Center of Research Excellence in Petroleum Refining and Petrochemicals at King Fahd University of Petroleum and Minerals (KFUPM). The authors thank J. Cejka and M. Kubu (Heyrovsky Institute of Physical Chemistry, Prague, Czech Republic) for providing zeolites TNU-9 and SSZ-33 and their characterization.

■ NOTATION

Ci	concentration of specie i in the riser simulator (mol/m^3)
CL	confidence limit
E_i	apparent activation energy of ith reaction (kJ/mol)
k_1	rate constant of reaction 1 (m^3/kg of catalyst·s) in the riser simulator
k_2	rate constant of reaction 2 (m^3/kg of catalyst·s) in the riser simulator
k_3	rate constant of reaction 3 (m^3/kg of catalyst·s) in the riser simulator
k_4	rate constant of reaction 4 (m^3/kg of catalyst·s) in the riser simulator
k	apparent kinetic rate constant (m^3/kg of catalyst·s) in the riser simulator
k_0	pre-exponential factor in Arrhenius equation defined at an average temperature [m^3/(kg of catalyst·s)], units based on first-order reaction in the riser simulator
k_i	apparent rate constant for the ith reaction in the fixed-bed reactor (s^{-1})
k_{oi}	pre-exponential factor for the ith reaction after reparameterization (s^{-1}) in the fixed-bed reactor
MWi	molecular weight of specie i
$MW_{dispro(avg)}$	average molecular weight of disproportionation products
R	universal gas constant (kJ/(kmol K)
t	reaction time (s)
t_τ	reaction time (s)
T	reaction temperature (K)
T_0	average temperature of the experiment
V	volume of the riser
W_c	mass of the catalysts
W_{hc}	total mass of hydrocarbons injected in the riser
F_{TM}	total mass flow rate (kg/min)
v_o	total volumetric flow rate (m^3/min)
y_i	mass fraction of ith component

Greek Letters

α	catalyst deactivation constant (TOS Model)
η	effectiveness factor, dimensionless

Subscripts

0	at time $t = 0$
1	for reaction 1
2	for reaction 2
3	for reaction 3
4	for reaction 4
cat	catalyst
i	for ith component

■ REFERENCES

(1) Cejka, J.; Wichterlova, B. Acid-catalyzed synthesis of mono-and dialkylbenzenes over zeolites: Active sites, zeolite Topology and reaction mechanisms. *Catal. Rev.* **2002**, *44*, 375–421.

(2) Tsai, T. C.; Liu, S. B.; Wang, I. Disproportionation and Transalkylation of alkylbenzenes over zeolite catalysts. *Appl. Catal., A* **1999**, *181*, 355–398.

(3) Chen, N. Y.; Garwood, W. E. Industrial application of shape-selective catalysis. *Catal. Rev.Sci. Eng.* **1986**, *28*, 185.

(4) Alberti, G. In *Solid-State Supramolecular Chemistry: Two- and Three-Dimensional Inorganic Networks*; Alberti, G., Bein, T., Eds.; Supramolecular Chemistry, Vol. 7; Lehn, J. M., Ed.; Pergamon: Elsevier Science: Amsterdam, 1996; Chapter 5.

(5) Degnan, T. F. Applications of zeolites in petroleum refining. *Top. Catal.* **2000**, *13*, 349–356.

(6) Maxwell, I. E. Zeolite catalysis in hydroprocessing technology. *Catal. Today* **1987**, *1*, 385–413.

(7) Burton, A.; Zones, S. Organic Molecules in Zeolite Synthesis; Their Preparation and Structure-Directing Effect. In *Introduction to Zeolite Science and Practice*, 3rd ed.; Cejka, J., Van Bekkum, H., Corma, A., Schuth, F., Eds.; *Stud. Surf. Sci. Catal.*, Vol. 68; Elsevier: Amsterdam, 2007; pp 137–179.

(8) Perego, C.; Ingallina, P. Recent advances in the industrial alkylation of aromatics: new catalysts and new processes. *Catal. Today* **2002**, *73*, 3–22.

(9) Wichterlova, B.; Cejka, J.; Zilkova, N. Selective synthesis of cumene and p-cumene over Al and Fe silicates with large and medium pore structures. *Microporous Mater.* **1996**, *6*, 405–414.

(10) Cejka, J.; Vondrova, A.; Wichterlova, B.; Vorbeck, G.; Fricke, R. The effect of Al, Fe, and in substitution in the MFI silicates structure on the aromatic hydrocarbon transformation-SI-OH-M site strength. *Zeolites* **1994**, *14*, 147–153.

(11) Zilkova, N.; Bejblova, M.; Gil, B.; Zones, S. I.; Burton, A. W.; Chen, C. Y.; Musilova-Pavlackova, Z.; Kosova, G.; Cejka, J. The role of the zeolite channel architecture and acidity on the activity and selectivity in aromatic transformations: The effect of zeolite cages in SSZ-35 zeolite. *J. Catal.* **2009**, *266*, 79–91.

(12) Rabiu, S.; Al-Khattaf, S. Kinetics of toluene methylation over ZSM-5 catalyst in a riser simulator. *Ind. Eng. Chem. Res.* **2008**, *47*, 39–47.

(13) Corma, A.; Llopis, F. J.; Martinez, C.; Sastre, G.; Valencia, S. The benefit of multipore zeolites: Catalytic behavior of zeolites with intersecting channels of different sizes for alkylation reactions. *J. Catal.* **2009**, *268*, 9–17.

(14) Carpenter, J. R.; Yeh, S.; Zones, S. I.; Davis, M. E. Further investigations on constraint index testing of zeolites that contain cages. *J. Catal.* **2010**, *269*, 64–70.

(15) Aneke, L. E.; Gerritsen, L. A.; van den Berg, P. J.; de Jong, W. A. The disproportionation of toluene over a HY/β-Al-F$_3$/Cu catalyst (1) Preparation and characterization. *J. Catal.* **1979**, *59*, 26–36.

(16) Borgna, A.; Sepulveda, J.; Magni, S. I.; Apesteguia, C. R. Active sites in the alkylation of toluene with methanol: A study by selective acid-base poisoning. *Appl. Catal., A: Gen.* **2004**, *276*, 207–215.

(17) Das, J.; Bhat, Y. S.; Bhardwaj, A. I.; Halgeri, A. B. Zeolite beta catalyzed C$_7$ and C$_9$ aromatics transformation. *Appl. Catal., A: Gen.* **1994**, *116*, 71–79.

(18) Zhu, Z.; Chen, Q.; Xie, Z.; Yang, Li, C. The roles of acidity and structure of zeolite for catalyzing toluene alkylation with methanol to xylene. *Microporous Mesoporous Mater.* **2006**, *88*, 16–21.

(19) Wang, I.; Tsai, T. C.; Huang, S. T. Disproportionation of toluene and trimethylbenzene and their transalkylation over zeolite Beta. *Ind. Eng. Chem. Res.* **1990**, *29*, 2005–2012.

(20) Dumitriu, E.; Hulea, V.; Kaliaguine, S.; Huang, M. M. Transalkylation of the alkylaromatic hydrocarbons in the presence of ultrastable Y zeolites; Transakylation of toluene with trimethylbenzenes. *Appl. Catal.* **1996**, *135*, 57–81.

(21) Wu, J. C.; Leu, L. J. Toluene disproportionation and transalkylation reaction over mordenite zeolite catalysts. *Appl. Catal.* **1983**, *7*, 283–294.

(22) Corma, A.; Costa-Vaya, V. I.; Diaz-Cabanas, M. J.; Llopis, F. J. Influence of pore-volume topology of zeolite ITQ-7 in alkylation and isomerization of aromatic compounds. *J. Catal.* **2002**, *207*, 46–56.

(23) Al-Khattaf, S.; Musilova-Pavlackova, Z.; Ali, M. A.; Cejka, J. Comparison of activity and selectivity of SSZ-33 based catalyst with other zeolites in toluene disproportionation. *Top. Catal.* **2009**, *52*, 140–147.

(24) Tsai, T. C.; Chen, W. H.; Lai, C. S.; Liu, S. B.; Wang, I.; Ku, C. S. Kinetics of toluene disproportionation over fresh and coked H-mordenite. *Catal. Today* **2004**, *97*, 297–302.

(25) Mikkenlsen, O.; Ronning, P.; Kolboe, S. Use of isotopic labeling for mechanistic studies of the methanol-to-hydrocarbons reaction. Methylation of toluene with methanol over H-ZSM-5, H-mordenite and H-beta. *Microporous Mesoporous Mater.* **2000**, *95*, 113.

(26) Llopis, F. J.; Sastre, G.; Corma, A. Xylene isomerization and aromatic alkylation in zeolites NU-87, SSZ-33, beta, and ZSM-5: molecular dynamics and catalytic studies. *J. Catal.* **2004**, *227*, 227–241.

(27) Emeis, C. A. Determination of integrated molar extinction coefficients for infrared absorption bands of pyridine adsorbed on solid acid catalysts. *J. Catal.* **1993**, *141*, 347–354.

(28) Gil, B.; Zones, S. I.; Hwang, S. J.; Bejblova, M. Cejka, Acdic properties of SSZ-33 and SSZ-35 novel zeolites: a complex infrared and MAS NMR study. *J. Phys. Chem.* **2008**, *112*, 2997–3007.

(29) de Lasa, H. I. Riser simulator for catalytic cracking studies. U.S. Patent 5, 1991, 102, 628.

(30) Kraemer, D. W. Ph.D. Dissertation, University of Western Ontario, London, Canada, 1991.

(31) Odedairo, T.; Al-Khattaf, S. Ethylation of benzene: Effect of zeolite acidity and structure. *Appl. Catal., A* **2010**, *385*, 31–45.

(32) Al-Khattaf, S. Catalytic transformation of toluene over a high acidity Y-zeolite based catalyst. *Energy Fuels* **2006**, *20*, 946–954.

(33) Cejka, J.; Kapustin, G. I.; Wichterlova, B. Factors controlling iso-selectivity/N-selectivity and para-selectivity in the alkylation of toluene with isopropanol on molecular sieves. *Appl. Catal., A* **1994**, *108*, 187–204.

(34) Venuto, P. B.; Landis, P. S. Organic synthesis over crystalline aluminosilicates. *Adv. Catal.* **1968**, *18*, 259–371.

(35) Kaeding, W. W.; Chu, C.; Young, L. B.; Weinstein, B.; Butter, S. A. Selective alkylation of toluene with methanol to produce paraxylene. *J. Catal.* **1981**, *67*, 159.

(36) Mirth, G.; Lercher, J. A. In situ IR Spectroscopic study of the surface species during methylation of toluene over HZSM-5. *J. Catal.* **1991**, *132*, 244–252.

(37) Ivanova, I. I.; Corma, A. An insitu C-13 MAS NMR study of toluene alkylation with methanol over H-ZSM-11. *Zeolites* **1995**, *97*, 27–34.

(38) Olsbye, U.; Tangstad, E.; Dahl, I. M. Partial oxidation of methane to synthesis gas in a fluidized bed reactor. *Stud. Surf. Sci. Catal.* **1994**, *81*, 303.

(39) Tomishige, K.; Matsuo, Y.; Yoshinaga, Y.; Sekine, Y.; Asadullah, M.; Fujimoto, K. Comparative study between fluidized bed and fixed bed reactors in methane reforming combined with methane combustion for the internal heta supply under pressurized condition. *Appl. Catal., A* **2002**, *223*, 225–238.

(40) Raj, K. J. A.; Padma Malar, E. J.; Vijayaraghavan, V. R. Shape selective reactions with AEL and AFI-type molecular sieves alkylation of benzene, toluene, and ethylbenzene with ethanol, 2-propanol, methanol and t-butanol. *J. Mol. Catal. A* **2006**, *243*, 99–105.

(41) Bhavikatti, S. S.; Patwardhan, S. R. Toluene disproportionation over nickel-loaded aluminium-deficient mordenite. 2. Kinetics. *Ind. Eng. Chem. Prod. Res. Dev.* **1981**, *20*, 106–109.

(42) Ouguan, X. U.; Hongye, S. U.; Jianbing, J. I.; JXiaoming, J. I. N.; Jian, C. H. U. Kinetic model and simulation analysis for toluene disproportionation and C_9 aromatics transalkylation. *Chin. J. Chem. Eng.* **2007**, *15*, 326–332.

(43) Wei, J. A mathematical theory of enhanced para-xylene selectivity in molecular-sieve catalysts. *J. Catal.* **1982**, *76*, 433–439.

(44) Comelli, R. A.; Canavese, S. A.; Querini, C. A.; Figoli, N. S. N.S. Coke deposition on platinum promoted WO_x-ZrO_2 during n-hexane isomerization. *Appl. Catal., A* **1999**, *182*, 275–283.

(45) Agarwal, A. K.; Brisk, M. L. Sequential experimental design for precise parameter estimation. 1. Use of reparameterization. *Ind. Eng. Chem. Process. Des. Dev.* **1985**, *24*, 203.

(46) Chang, J. R.; Sheu, F. C.; Cheng, Y. M.; Wu, J. C. Kinetics and optimization of the toluene disproportionation reaction over solid acid catalysts. *Appl. Catal.* **1987**, *33*, 39–53.

(47) Levenspiel, O. *Chemical Reaction Engineering*, 3rd ed.; John Wiley & Sons: New York, 1999.

(48) Odedairo, T.; Al-Khattaf, S. Kinetic analysis of benzene ethylation over ZSM-5 based catalyst in a fluidized-bed reactor. *Chem. Eng. J.* **2010**, *157*, 204–15.

(49) Odedairo, T.; Al-Khattaf, S. Kinetic investigation of benzene ethylation with ethanol over USY zeolite in a riser simulator. *Ind. Eng. Chem. Res.* **2010**, *49*, 1642–1651.

(50) Ko, A.; Kuo, C. T. Isomerization and disproportionation of 1,2,4-trimethylbenzene over HY zeolite. *J. Chin. Chem. Soc.* **1994**, *41*, 141–150.

(51) Al-Khattaf, S.; Tukur, N. M.; Al-Amer, A. 1,2,4-Tirmethylbenzene transformation reaction compared with its transalkylation reaction with toluene over USY zeolite catalyst. *Ind. Eng. Chem. Res.* **2007**, *46*, 4459–4467.

(52) Mantha, R.; Bhatia, S.; Rao, M. S. Kinetics of deactivation of methylation of toluene over H-ZSM-5 and hydrogen mordenite catalyst. *Ind. Eng. Chem. Res.* **1991**, *30*, 281–286.

(53) Bhat, Y. S.; Halgeri, A. B.; Prasada Rao, T. S. R. Kinetics of toluene alkylation with methanol on H-ZSM-8 zeolite catalyst. *Ind. Eng. Chem. Res.* **1989**, *28*, 890–894.

(54) Mirth, G.; Lercher, J. A. Coadsorption of toluene and methanol on H-ZSM-5 zeolites. *J. Phys. Chem.* **1991**, *95*, 3736–3740.

(55) Karger, J.; Ruthven, D. M. *Diffusion in zeolites and other microporous solids*; Wiley: New York, 1992.